

Importance of non-first-order effects in the $(e,3e)$ double ionization of helium

A. Lahmam-Bennani,¹ A. Duguet,¹ C. Dal Cappello,² H. Nebdi,³ and B. Piraux³

¹Laboratoire des Collisions Atomiques et Moléculaires (UMR 8625), Bât 351, Université Paris XI, F-91405 Orsay Cedex, France

²Institut de Physique, Laboratoire de Physique Moléculaire et des Collisions, Technopôle 2000, 1 rue Arago, F-57078 Metz Cedex 03, France

³Laboratoire de Physique Atomique et Moléculaire, Université Catholique de Louvain, Chemin du Cyclotron, 2 B-1348 Louvain-la-Neuve, Belgium

(Received 31 May 2002; published 17 January 2003)

Angular distributions of the two ejected electrons resulting from the double ionization of helium by electron impact have been measured by means of a multicoincidence multiangle $(e,3e)$ spectrometer at an incident energy of about 0.6 keV and equal outgoing energies $E_b = E_c = 11$ eV. We identify various regimes of kinematical parameters where substantial differences are found with respect to the first-Born convergent close-coupling calculations: an angular shift of the position of the main lobe and the presence of additional lobes. These differences are attributed to high-order contributions in the projectile-target interaction. This conclusion is supported by recent $(e,3e)$ calculations performed within the second-Born approximation.

DOI: 10.1103/PhysRevA.67.010701

PACS number(s): 34.80.Dp

The investigation of the correlated fragmentation dynamics of an atomic system under photon or charged particle impact is one of the most challenging problems addressed in modern atomic physics. In the last few years, kinematically complete experiments based on multicoincidence and multi-angle detection of all the final-state particles have been developed. This, in conjunction with the theoretical progress, has allowed a rather good understanding of the very basic three-body fragmentation processes, such as electron impact single ionization [the so-called $(e,2e)$ reaction] [1] or $(\gamma,2e)$ photo-double-ionization process [2]. In contrast, a detailed knowledge about the N -body problem ($N > 3$) is only slowly being gained due to its theoretical as well as experimental complexity. The most basic N -body process is the electron-impact double ionization (DI) of helium,—the so called $(e,3e)$ reaction, since helium is the simplest two-electron system that yields a pure four-body problem in the final state, namely, a He^{2+} bare ion and three electrons.

Experimental $(e,3e)$ results on He have recently been published for the first time by Taouil *et al.* (Ref. [3]) and subsequently by Dorn *et al.* [4], soon followed by a number of new experimental results (Refs. [5–9]). In these studies, the energy of both the projectile and the fast scattered electrons was deliberately chosen to be very large, respectively, ~ 5.5 keV, ~ 2 keV, and ~ 1 keV. This was justified by the *a priori* idea that a simple picture where the DI process is viewed as being due to a single interaction of the projectile with the target can be adopted. It was therefore natural that almost all the theoretical treatments proposed so far [5,6,10] to describe the experimental results made use of the first-Born (FB) approximation. Roughly, these calculations yield a good agreement with the experiment as to the general features (dips and peaks) present in the angular distributions. However, even at the highest incident energy, 5.5 keV, some puzzling disagreements with the *absolute* experimental data were reported [6], concerning both the magnitude and the shape of the cross section. These were at least partly attributed to contributions which go beyond first order in the projectile-target interaction and which are not included in the

first-Born approximation (FBA). Such conclusion was also clearly suggested by the Faddeev-type approach of Berakdar [11]. Despite this, there remains a doubt as to the reality of the breakdown of the FBA for DI at 1–5-keV impact energy, mostly because it is widely acknowledged that the FBA does hold for $(e,2e)$ single ionization (SI) [12,13]. In Dorn *et al.* experiments at lower impact energy, 2 keV [8,9], a symmetry breaking of the cross section with respect to the direction of the momentum transfer is observed. This is a clear signature of non-first-Born interactions. At the higher energy of 5.5 keV, similar symmetry breakings were reported for Ar and Ne [14,15], but could not be observed for He [6] due to the limited range of the experimental data. The relative results of Dorn *et al.*'s *relative* results were presented as 2D density plots of the $(e,3e)$ cross section over the “full” collision plane. Such global pictures are very helpful for qualitative comparison with the theoretical models, and for visualizing the overall structure of the cross section (extrema, nodes, symmetry lines). However, they do not reveal subtle details as do the “individual” cuts obtained in the fixed ejected angle plots. Further experiments on He at even lower impact energy, 1.1 keV [7], emphasized “the large role played by non-first-Born processes.” The next step in the investigation of these non-first-Born effects was made by Jia *et al.* [16]. In their $(e,3e)$ measurements on Ar at 560-eV collision energy, they observe that these effects are enhanced with respect to former experiments [14,15]; there is not only the symmetry breaking about the direction of the momentum transfer, but also a strong modification of the “global” in-plane distribution of the cross section and the appearance of a new small structure near the main ones. This prompted us for a reinvestigation of the He case at a comparable low-collision energy to find out whether or not similar strong modifications do also occur. One of the questions we address here is to what extent the origin of these deviations could be understood within models that include non-first-Born effects [17].

We present here the data from a new $(e,3e)$ experiment on He performed at a low incident energy, 601 eV, the other kinematical parameters being similar to those utilized in

Refs. [5,7]. At this low incident energy, second or higher-order effects are expected to be enhanced. The data are compared to those obtained by using first- and second-Born treatments [17] including the accurate first-Born convergent-close-coupling (CCC) calculations [6,7]. The comparison between the experimental data and the theories allows to clearly attribute some of the features identified in the angular distributions (rotation of the main lobe), to second-order contributions in the projectile-target interaction. It also gives an evidence that these effects are very strong, much stronger than they are known to be in $(e,2e)$ SI under similar impact energy.

The data have been collected employing a $(e,3e)$ spectrometer whose essential feature is the in-plane multicoincidence and multiangle detection of both ejected electrons using two-twin double toroidal analyzers equipped with position sensitive detectors. The experimental setup and procedure have been described elsewhere [6,18]. Briefly, the incident electron beam ($E_0=601\pm 1$ eV) crosses at right angle the target gas beam. The fast scattered electron ($E_a=500$ eV) is energy analyzed in a cylindrical analyzer (energy resolution $\Delta E_a=\pm 1.5$ eV) and detected on a channeltron at a fixed angle ($\theta_a=+1.5^\circ$), corresponding to fixed momentum-transfer vector, $K=0.61$ au, in the direction $\theta_K=-15^\circ$. The value of the scattering angle is measured with an accuracy of $\pm 0.02^\circ$, whereas the spectrometer acceptance angle is $\Delta\theta_a=\pm 0.10^\circ$. Hence, a high-momentum-transfer resolution ($\Delta K=\pm 0.006$ au) and a small uncertainty in the momentum transfer direction ($< \pm 0.9^\circ$) are achieved. The ejected electrons ($E_b=E_c=11$ eV) are collected by the toroidal analyzers in the collision plane (\vec{k}_0, \vec{k}_a), over the useful angular ranges $20^\circ \leq \theta_b \leq 160^\circ$ and $200^\circ \leq \theta_c \leq 340^\circ$. Throughout this paper, positive scattering and ejection angles are measured counterclockwise, starting at the incident-beam direction, and are allowed to vary between 0 and 360° . The energy and angle resolutions for the ejected electrons are fixed in the off-line analysis [18] to $\Delta E_b=\Delta E_c=\pm 2$ eV, and $\Delta\theta_b=\Delta\theta_c=\pm 5^\circ$. As far as the present contribution is concerned, the registered triple coincidence events are sorted in the so-called “ θ -variable mode” either at fixed θ_b and varying θ_c , or vice versa.

The $(e,3e)$ fivefold differential cross section (FDCS), the most differential one, is given by

$$\frac{d^5\sigma}{d\Omega_a d\Omega_b d\Omega_c dE_b dE_c} = \frac{(2\pi)^4}{k_0} k_a k_b k_c |T_{fi}|^2, \quad (1)$$

where \vec{k}_0, \vec{k}_a are the initial and final momenta of the (fast) incident electron. \vec{k}_b, E_b and \vec{k}_c, E_c are the momentum and the energy of the ejected electrons. T_{fi} is the on-the-energy-shell T -matrix element. Exchange between the fast incident electron and the target ones is neglected. We write the T -matrix element as a sum of the first- and the second-Born terms as follows:

$$\begin{aligned} T_{fi} = & (2\pi)^{-3} \langle \Phi_{\vec{k}_b, \vec{k}_c}(\vec{r}_1, \vec{r}_2) | \langle e^{i\vec{k}_a \cdot \vec{r}_0} | V_d | e^{i\vec{k}_0 \cdot \vec{r}_0} \rangle | \Phi_i(\vec{r}_1, \vec{r}_2) \rangle \\ & + \frac{2}{(2\pi)^6} \lim_{\epsilon \rightarrow 0^+} \sum_{\gamma} \int d\vec{k}_{\gamma} \frac{1}{k_0^2 - k_{\gamma}^2 - 2(E_{\gamma} - E_{1S}) + i\epsilon} \\ & \times \langle \Phi_{\vec{k}_b, \vec{k}_c}(\vec{r}_1, \vec{r}_2) | \langle e^{i\vec{k}_a \cdot \vec{r}_0} | V_d | e^{i\vec{k}_{\gamma} \cdot \vec{r}_0} \rangle | \Phi_{\gamma}(\vec{r}_1, \vec{r}_2) \rangle \\ & \times \langle \Phi_{\gamma}(\vec{r}_1, \vec{r}_2) | \langle e^{i\vec{k}_{\gamma} \cdot \vec{r}_0} | V_d | e^{i\vec{k}_0 \cdot \vec{r}_0} \rangle | \Phi_{1S}(\vec{r}_1, \vec{r}_2) \rangle. \quad (2) \end{aligned}$$

V_d represents the direct interaction between the fast incident electron and the target. It is given by $1/r_{01} + 1/r_{02} - 2/r_0$; \vec{r}_0 is the coordinate of the incident electron while \vec{r}_1 and \vec{r}_2 refer to the coordinates of the initially bound electrons and $r_{01}=|\vec{r}_0-\vec{r}_1|$, $r_{02}=|\vec{r}_0-\vec{r}_2|$. The fast electron which interacts twice with the target has a momentum \vec{k}_{γ} after the first interaction. This introduces a new favored direction in addition to the momentum transfer $\vec{K}=\vec{k}_0-\vec{k}_a$. It is this new direction which is responsible for the breaking of the symmetry with respect to the momentum transfer. Φ_i and $\Phi_{\vec{k}_b, \vec{k}_c}$ are the initial and final target state wave functions. Here, Φ_i is a reasonably accurate ground-state wave function of helium [17] of energy E_{1S} , while $\Phi_{\vec{k}_b, \vec{k}_c}$ is a (symmetrized) product of two Coulomb wave functions times the usual Gamow factor that takes into account, though approximately, the electron-electron correlation. Φ_{γ} is an intermediate target state of energy E_{γ} . The summation over γ includes an integral over the single and double continua of helium whose calculation stays an extremely challenging theoretical problem. In order to bypass this difficulty, one usually replaces the factor $E_{\gamma} - E_{1S}$ by a so-called average excitation energy \bar{w} and use the closure relation to perform the summation over γ . Unless it is possible to identify a few dominant intermediate target states, the choice of \bar{w} is very delicate because the results may significantly change with \bar{w} . In the present case, we used this closure approximation and checked that within our approximation for the final-state wave function, the main effects of the second-order contributions remain qualitatively the same irrespective of \bar{w} although their amplitude changes. We have also performed the second-order Born calculations where we used a very accurate ground-state wave function [19] and the same final-state wave function as above; the results are in fair agreement with the second-Born results presented here.

In the following, we present filled contour plots of the $(e,3e)$ FDCS over the full collision plane for the same kinematical arrangement as in the experiment. In Fig. 1, we show the experimental results, in Fig. 2, our first-Born results [first term of the rhs of Eq. (2)] and in Fig. 3, our second-Born results [Eq. (2)]. Our first-Born results exhibit two peaks. These peaks are found on a symmetry axis (dashed line) whose existence corresponds to both electrons being ejected symmetrically with respect to the momentum transfer: $\theta_b - \theta_K = -(\theta_c - \theta_K)$. A similarly filled contour plot (not shown here) is obtained by using the FB-CCC data with one important difference: in the FB-CCC results, the amplitude of the upper peak around $\theta_b=90^\circ$ and $\theta_c=230^\circ$ is lower

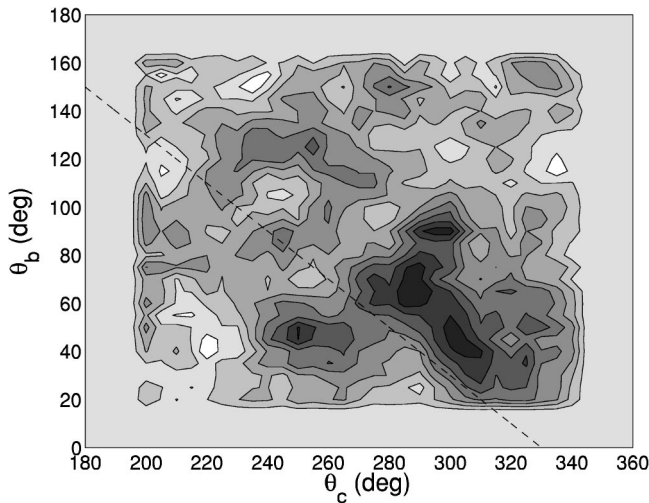


FIG. 1. Filled contour plot of the experimental ($e,3e$) FDCS data as a function of θ_b and θ_c . $E_0=601$ eV and $E_b=E_c=11$ eV. $\theta_a=1.5^\circ$. The dark zones are associated with the highest values. The first-Born symmetry axis (dashed line) is also shown.

than the amplitude of the lower peak around $\theta_b=50^\circ$ and $\theta_c=280^\circ$ by contrast to our first-Born results. This difference results from a better description of the electron-electron correlation in the final channel in the FB-CCC calculations. The experimental data shown in Fig. 1 do not fulfill the above reflection symmetry, meaning that θ_K is not anymore a favored direction. They also show, as it was the case for Ar at similar energy (Ref. [16]) a strong modification of the overall in-plane distribution of the cross section: on one hand, they do not even exhibit the upper peak; on the other hand, the lower peak is elongated with respect to the first-Born results, both along the above symmetry axis and perpendicular to it; it is made of various maxima, the largest one at around $\theta_b=60^\circ$ and $\theta_c=280^\circ$ corresponds roughly to the peak position in the first-Born theoretical results, though being strongly shifted upwards. Furthermore, we note the appearance of three new peaks: two of them appear on each side of the above symmetry axis, though not symmetrically at around

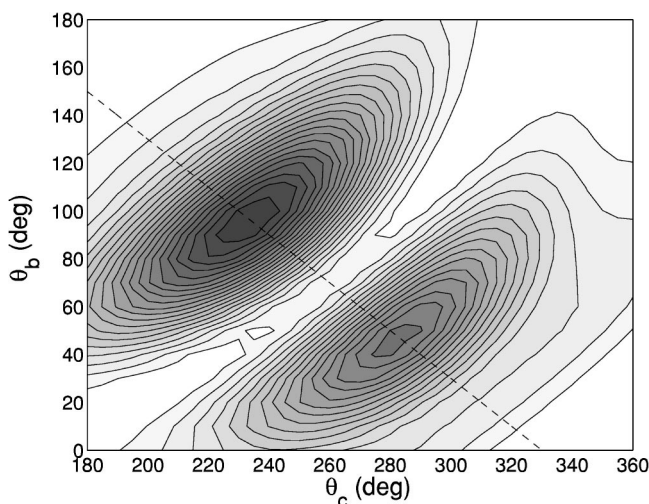


FIG. 2. Same as Fig. 1 but for our first-Born results.

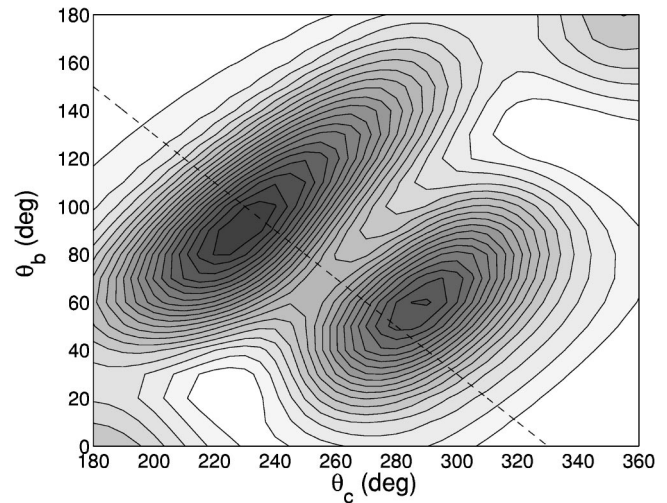


FIG. 3. Same as Fig. 1 but for our second-Born results.

$\theta_b=45^\circ$ and $\theta_c=250^\circ$ and around $\theta_b=90^\circ$ and $\theta_c=290^\circ$, whereas the third one appears more or less along this axis at around $\theta_b=40^\circ$ and $\theta_c=300^\circ$. Taking into account the fact that the experimental data are relative, the existence of the three additional peaks allows to identify three angular regions where high-order effects are expected to be important. Clearly, the second-Born contributions we calculated are not sufficient to explain all these effects (see Fig. 3). However, in the first angular regime (around $\theta_b=60^\circ$ and $\theta_c=280^\circ$), we observe in Fig. 3 that the second-Born results are in better agreement with the experimental data than the first-Born ones, the main peak being shifted by about 20° above the symmetry axis. In the following, we analyze this effect more quantitatively by studying the ($e,3e$) angular distribution for θ_c fixed and equal to 280° i.e., the value where the first-Born results are peaking. This angular distribution is presented in

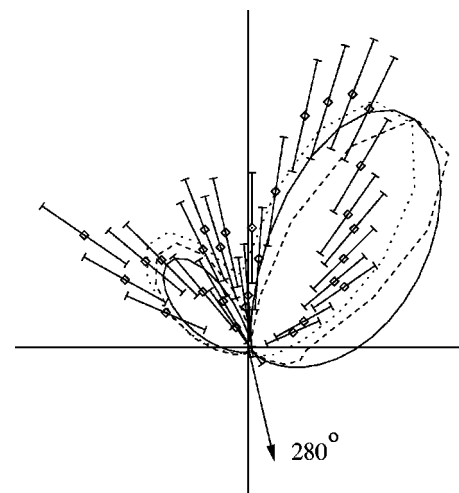


FIG. 4. Relative ($e,3e$) angular distribution for He for $E_0=601$ eV and $E_b=E_c=11$ eV. A coplanar geometry is considered with $\theta_a=1.5^\circ$ and $\theta_c=280^\circ$. Open squares, experiments. Full line, FB-CCC results. Dotted line, B2 results. Dashed line, our B1 results. All results are normalized so that the amplitudes of the main peak coincide.

Fig. 4 where we compare the experimental data to the FB-CCC [21] and our first- and second-Born results. At the first glance, the first-order models seem to reproduce the gross features of the experimental distribution, that is the existence of the main lobe and a secondary one located in two roughly perpendicular directions at about 60° and 150° and separated by a deep if not a zero minimum corresponding to the back-to-back emission of the electrons. This minimum is reminiscent of the angular distributions observed in PDI [20] or in high-energy ($e,3e$) distributions [6] where the shape of the distribution is mostly imposed by the dipole selection rule which forbids back-to-back emission under photon. impact due to the $^1P^0$ symmetry of the wave function describing the pair of outgoing electrons in the ionization of He. However, a closer inspection of Fig. 4 shows several significant differences between the (relative) experimental data and the first-Born results (i) the secondary lobe in the theory has in fact a double-lobe structure in the experiment whose origin is still unexplained, (ii) the direction of the main experimental lobe is shifted backwards by about 20° and (iii), this lobe is narrower than the first-Born predictions with a full width at half maximum of about 35° and 45° , respectively. The features (ii) and (iii), in particular, bear an obvious resemblance with previous observations made in ($e,2e$) single-ionization studies [22] which strongly suggests that these effects could be

attributed to the presence of large non-first-order contributions in the projectile-target interaction. In the present case, the shift of the main experimental peak is partially reproduced by our second-Born results. As mentioned before, this shift results from the fact that since the fast electron interacts twice with the target, it undergoes two transfers of momentum introducing a second favored direction in the problem in addition to the direction of the momentum transfer $\vec{K} = \vec{k}_0 - \vec{k}_a$. It is the reason why all first-order calculations are unable to reproduce the shift of the main experimental peak even if as in the case of FB-CCC, the target electron correlation in the final state is treated at all orders. The second peak at about 150° depends significantly on the type of approximation which is used. However, this peak does not seem to be shifted in the second-Born calculations. This suggests that the amplitude of this peak depends also on how the correlation between the target electrons is treated in the final state.

The present analysis clearly demonstrates the importance of high-order effects in ($e,3e$) processes. In particular, we have identified a regime of kinematical parameters where second-order effects are very significant.

The authors acknowledge Dr. A. Kheifets for providing them with the results of the CCC calculations.

-
- [1] T.N. Rescigno, M. Baertschy, W.A. Isaacs, and C.W. McCurdy, *Science* **286**, 2474 (1999).
- [2] J.S. Briggs and V. Schmidt, *J. Phys. B* **33**, R1 (2000).
- [3] I. Taouil, A. Lahmam-Bennani, A. Duguet, M. Lecas, and L. Avaldi, *Phys. Rev. Lett.* **81**, 4600 (1998).
- [4] A. Dorn, R. Moshhammer, C.D. Schröter, T.J.M. Zouros, W. Schmitt, H. Kollmus, R. Mann, and J. Ullrich, *Phys. Rev. Lett.* **82**, 2496 (1999).
- [5] A. Lahmam-Bennani, I. Taouil, A. Duguet, M. Lecas, L. Avaldi, and J. Berakdar, *Phys. Rev. A* **59**, 3548 (1999).
- [6] A. Kheifets, I. Bray, A. Lahmam-Bennani, A. Duguet, and I. Taouil, *J. Phys. B* **32**, 5047 (1999).
- [7] A. Lahmam-Bennani, A. Duguet, M.N. Gaboriaud, I. Taouil, M. Lecas, A. Kheifets, J. Berakdar, and C. Dal Cappello, *J. Phys. B* **34**, 3073 (2001).
- [8] A. Dorn, A. Kheifets, C.D. Schröter, B. Najjari, C. Höhr, R. Moshhammer, and J. Ullrich, *Phys. Rev. Lett.* **86**, 3755 (2001).
- [9] A. Dorn, A. Kheifets, C.D. Schröter, B. Najjari, C. Höhr, R. Moshhammer, and J. Ullrich, *Phys. Rev. A* **65**, 032709 (2002).
- [10] A. Kheifets, I. Bray, J. Berakdar, and C. Dal Cappello, *J. Phys. B* **35**, L15 (2002).
- [11] J. Berakdar, *Phys. Rev. Lett.* **85**, 4036 (2000).
- [12] H. Ehrhardt, K. Jung, H. Klar, A. Lahmam-Bennani, and P. Schlemmer, *J. Phys. B* **20**, L193 (1987).
- [13] A. Lahmam-Bennani, *J. Phys. B* **24**, 2401 (1991).
- [14] B. El Marji, C. Schröter, A. Duguet, A. Lahmam-Bennani, M. Lucas, and L. Spielberger, *J. Phys. B* **30**, 3677 (1997).
- [15] C. Schröter, B. El Marji, A. Lahmam-Bennani, A. Duguet, M. Lucas, and L. Spielberger, *J. Phys. B* **31**, 131 (1998).
- [16] C.C. Jia, A. Lahmam-Bennani, A. Duguet, L. Avaldi, M. Lecas, and C. Dal Cappello, *J. Phys. B* **35**, 1103 (2002).
- [17] M. Grin, C. Dal Cappello, R. El Mkhanter, and J. Rasch, *J. Phys. B* **33**, 131 (2000).
- [18] A. Duguet, A. Lahmam-Bennani, M. Lecas, and B. El Marji, *Rev. Sci. Instrum.* **69**, 3524 (1998).
- [19] G. Lagmago-Kamta, B. Piraux, and A. Scrinzi, *Phys. Rev. A* **63**, 040502 (2001).
- [20] A. Huetz, P. Selles, D. Waymel, and J. Mazeau, *J. Phys. B* **24**, 1917 (1991).
- [21] A. Kheifets (private communication).
- [22] H. Ehrhardt, K. Jung, G. Knoth, and P. Schlemmer, *Z. Phys. D: At., Mol. Clusters* **1**, 3 (1986).